PERGAMON

Mathematical and Computer Modelling 36 (2002) 259–273

MATHEMATICAL AND COMPUTER MODELLING

www.elsevier.com/locate/mcm

Discontinuous Bifurcations of Periodic Solutions

R. I. LEINE AND D. H. VAN CAMPEN
Department of Mechanical Engineering
Eindhoven University of Technology
P. O. Box 513, 5600 MB Eindhoven, The Netherlands
R.I.Leine@tue.nl

Abstract—This paper discusses different aspects of bifurcations of periodic solutions in discontinuous systems. It is explained how jumps in the fundamental solution matrix lead to jumps of the Floquet multipliers of periodic solutions. A Floquet multiplier of a discontinuous system can jump through the unit circle causing a discontinuous bifurcation. Numerical examples show discontinuous fold and symmetry-breaking bifurcations. The discontinuous fold bifurcation can connect stable branches to branches with infinitely unstable periodic solutions.

Keywords—Discontinuous, Bifurcation, Stick-slip, Dry friction.

1. INTRODUCTION

The aim of this paper is to explain how discontinuous bifurcations of periodic solutions arise in systems with a discontinuous vector field.

During the last decade many textbooks about bifurcation theory for smooth systems appeared and bifurcations of periodic solutions in smooth systems are well understood [1–4]. However, little is known about bifurcations of periodic solutions in discontinuous systems. Discontinuous dynamical systems arise due to physical discontinuities such as dry friction, impact, and backlash in mechanical systems or diode elements in electrical circuits. Many publications deal with discontinuous systems [5–21]. Most of the published bifurcation diagrams were constructed from data obtained by brute force techniques and only show stable branches, whereas those made by path-following techniques do show bifurcations to unstable solutions, but the bifurcations behave smoothly and are not discontinuous. Recently, Yoshitake and Sueoka [22] and Yoshitake *et al.* [23] studied different discontinuous systems and presented bifurcation diagrams which show discontinuous bifurcations. The Floquet multipliers expose jumps at the discontinuous bifurcation points [22].

Andronov *et al.* [24] treat periodic solutions of discontinuous systems. They revealed many aspects of discontinuous systems but did not treat discontinuous bifurcations with regard to Floquet theory.

This project was supported by the Dutch Technology Foundation, STW. The authors are much indebted to B.L. Van de Vrande for useful comments.

0895-7177/02/$ - see front matter Typeset by $\mathcal{A}_{\mathcal{M}}\mathcal{S}$-TEX
PII: S0895-7177(02)00124-3

Before proceeding we should clarify what we mean with the term *'discontinuous system'*. Discontinuous systems can be divided into three types according to their degree of discontinuity.

(1) Systems with a discontinuous Jacobian, like systems with purely elastic supports. Those systems have a continuous vector field, but the vector field is nonsmooth.
(2) Systems described by differential equations with a discontinuous right-hand side (also called Filippov systems [25,26]). The vector field is discontinuous of those systems. Examples are systems with viscoelastic supports and dry friction.
(3) Systems which expose discontinuities in the state, like impacting systems with velocity reversals. This type of system is not treated in this paper (see [27]).

The theory of bifurcations in smooth dynamical systems is well developed. This is not the case for bifurcations in discontinuous dynamical systems. In this paper, we will study bifurcations of periodic solutions in systems with a discontinuous right-hand side (Filippov systems).

The objective of the paper is to demonstrate different aspects of *discontinuous bifurcation*, which is a novel, nonclassical type of bifurcation. The basic idea is that Floquet multipliers of discontinuous systems can jump when a parameter of the system is varied. If a Floquet multiplier jumps through the unit circle (Figure 1), a discontinuous bifurcation is encountered. The idea of a discontinuous bifurcation of a periodic solution, at which a Floquet multiplier jumps through the unit circle, is similar to the 'C-bifurcations' in the work of Feigin [28–30] and di Bernardo *et al.* [31–33]. Feigin classifies C-bifurcations on the number of real-valued eigenvalues of the Poincaré map that are smaller than -1 or larger than $+1$, but does not take complex eigenvalues into account. Nonclassical bifurcations of nonsmooth mappings were also addressed by Nusse and York [34]. In this paper, it is explained how the discontinuous bifurcations come into being through jumps of the fundamental solution matrix. It is shown that the fundamental solution matrix can jump if a periodic solution touches a nonsmooth hypersurface of discontinuity.

Although there exist different definitions for a bifurcation, we will take the definition of Seydel [4] that at a bifurcation point, the number of fixed points or (quasi-)periodic solutions changes for a varying system parameter. Bifurcations which expose a jump of the Floquet multipliers are called *discontinuous bifurcations*.

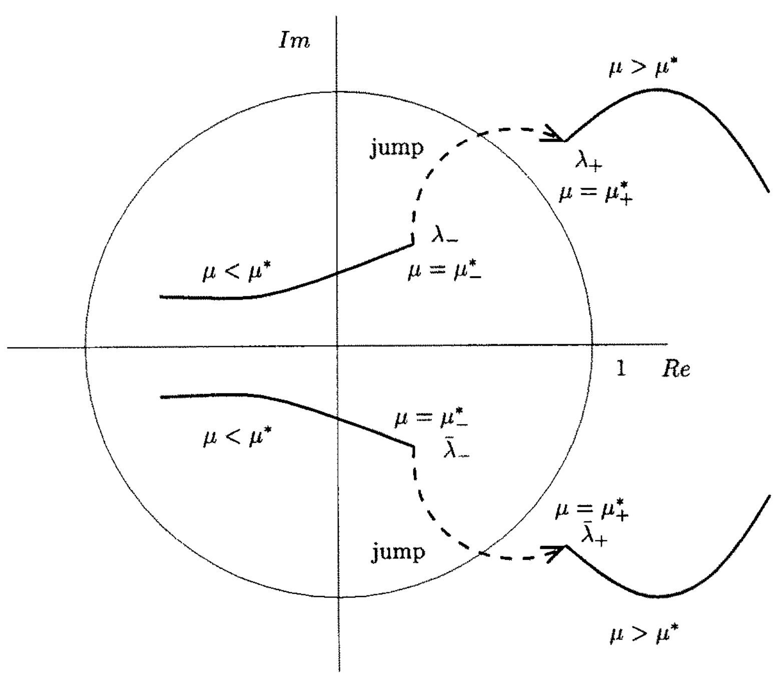

Figure 1. Discontinuous bifurcation.

Three examples of discontinuous bifurcations of periodic solutions are discussed in the next sections, and it is explained how discontinuous bifurcations come into being through Floquet theory. The first example is a trilinear spring system which shows a discontinuous fold bifurcation connecting a stable branch to an unstable branch. A stick-slip system is treated in the second example. The discontinuous fold bifurcation connects a stable branch to an infinitely unstable branch. The discontinuous symmetry-breaking bifurcation will be discussed in Section 4. The results obtained for those examples demonstrate the need to enlarge the bifurcation theory for smooth systems to the greater class of Filippov systems.

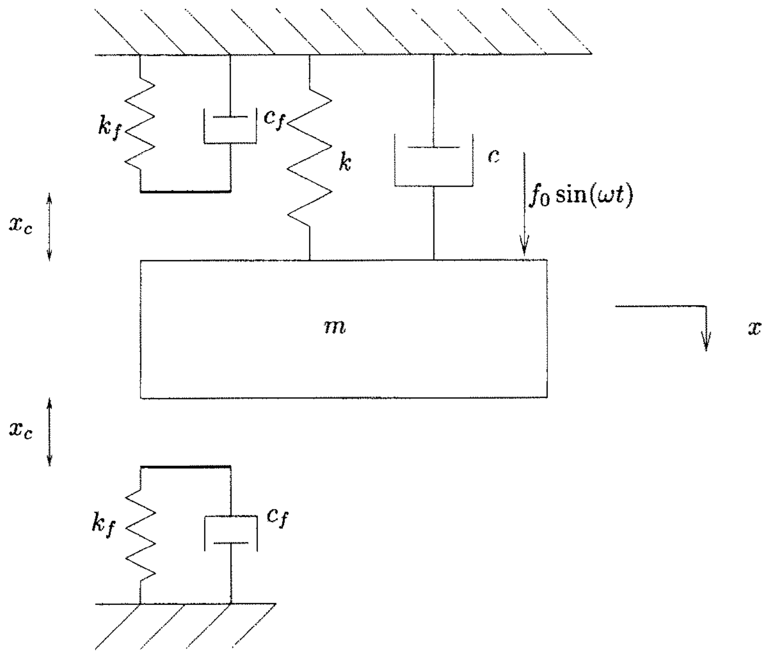

Figure 2. Trilinear system.

2. TRILINEAR SPRING SYSTEM

In this section, we will treat a discontinuous fold bifurcation arising in a trilinear spring system (Figure 2).

The forced oscillation of a damped mass on a spring with cubic term leads to the Duffing equation [1,2,35,36]. The Duffing equation is the classical example where the backbone curve of the harmonic peak is bent and two folds (also called turning point bifurcations) are born. In our example, we will consider a similar mass-spring-damper system, where the cubic spring is replaced by a trilinear spring. Additionally, trilinear damping is added to the model. The trilinear damping will turn out to be essential for the existence of a *discontinuous* fold bifurcation.

The model is very similar to the model of Natsiavas [37,38], but the transitions from contact with the support to no contact are different from those in the model of Natsiavas. The model of Natsiavas switches as the position of the mass passes the contact distance (in both transition directions). In our model, contact is made when the position of the mass passes the contact distance (for growing $|x|$), and contact is lost when the contact force becomes zero.

We consider the system depicted in Figure 2. The model has two supports on equal contact distances x_c. The supports are first-order systems which relax to their original state if there is no contact with the mass. If we assume that the relaxation time of the supports is much smaller than the time interval between two contact events, we can neglect the influence of free motion of the supports. It is therefore assumed that the supports are at rest at the moment that contact is made. This is not an essential assumption but simplifies our treatment as the system reduces to a second-order equation. The second-order differential equation of this system is

$$m\ddot{x} + C(\dot{x}) + K(x) = f_0 \sin(\omega t), \tag{1}$$

where

$$K(x) = \begin{cases} kx, & [x, \dot{x}]^{\top} \in V_{-}, \\ kx + k_f(x - x_c), & [x, \dot{x}]^{\top} \in V_{+1}, \\ kx + k_f(x + x_c), & [x, \dot{x}]^{\top} \in V_{+2}, \end{cases} \tag{2}$$

is the trilinear restoring force and

$$C(\dot{x}) = \begin{cases} c\dot{x}, & [x, \dot{x}]^{\top} \in V_{-}, \\ (c + c_f)\dot{x}, & [x, \dot{x}]^{\top} \in V_{+1} \cup V_{+2}, \end{cases} \tag{3}$$

is the trilinear damping force. The state space is divided into three subspaces V_-, V_{+1}, and V_{+2} (Figure 3).

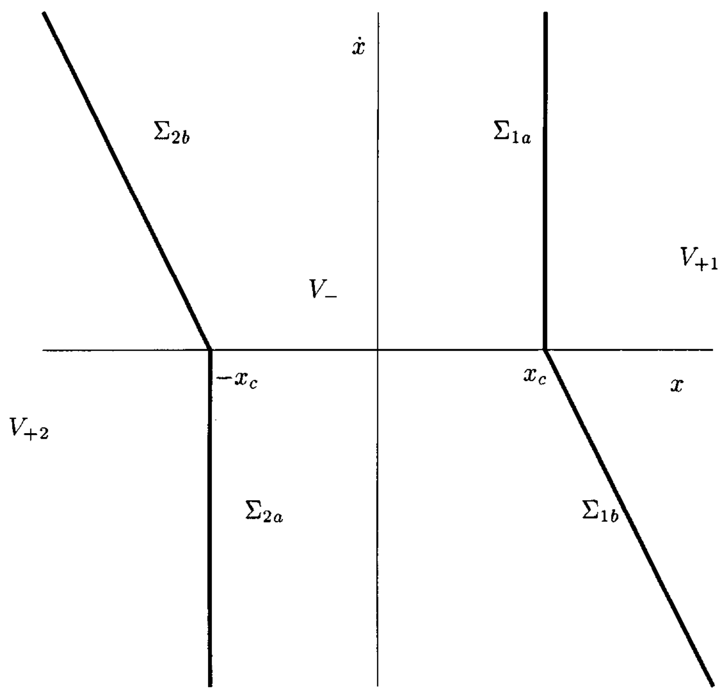

Figure 3. Subspaces of the trilinear system.

If the mass is in contact with the lower support, then the state is in space V_{+1}

$$V_{+1} = \left\{ [x, \dot{x}]^{\top} \in \mathbb{R}^2 \mid x > x_c,\ k_f(x - x_c) + c_f\dot{x} \geq 0 \right\},$$

whereas if the mass is in contact with the upper support, then the state is in space V_{+2}

$$V_{+2} = \left\{ [x, \dot{x}]^{\top} \in \mathbb{R}^2 \mid x < -x_c,\ k_f(x + x_c) + c_f\dot{x} \leq 0 \right\}.$$

If the mass is not in contact with one of the supports, then the state is in space V_- defined by

$$V_- = \left\{ [x, \dot{x}]^{\top} \in \mathbb{R}^2 \mid [x, \dot{x}]^{\top} \notin (V_{+1} \cup V_{+2}) \right\}.$$

We define the indicator functions $h_{1a}(x, \dot{x})$ and $h_{1b}(x, \dot{x})$ as

$$h_{1a}(x, \dot{x}) = x - x_c, \tag{4}$$

$$h_{1b}(x, \dot{x}) = k_f(x - x_c) + c_f \dot{x}. \tag{5}$$

The hypersurface Σ_1 between V_- and V_{+1} consists of two parts Σ_{1a} and Σ_{1b}. The part Σ_{1a} defines the transition from V_- to V_{+1} because contact is made when x becomes larger than x_c.

$$\Sigma_{1a} = \left\{ [x, \dot{x}]^\top \in \mathbb{R}^2 \mid h_{1a}(x, \dot{x}) = 0,\ h_{1b}(x, \dot{x}) \geq 0 \right\}. \tag{6}$$

The part Σ_{1b} is defined by the indicator equation which defines the transition from V_{+1} back to V_- as contact is lost when the support-force becomes zero (the support can only push, not pull on the mass).

$$\Sigma_{1b} = \left\{ [x, \dot{x}]^\top \in \mathbb{R}^2 \mid h_{1a}(x, \dot{x}) \geq 0,\ h_{1b}(x, \dot{x}) = 0 \right\}. \tag{7}$$

Similarly, the hyper-surface Σ_2 between V_- and V_{+2} consists of two parts Σ_{2a} and Σ_{2b} defined by the indicator equations

$$h_{2a}(x, \dot{x}) = x + x_c, \tag{8}$$

$$h_{2b}(x, \dot{x}) = k_f(x + x_c) + c_f \dot{x}. \tag{9}$$

Discontinuous systems exhibit discontinuities (or 'saltations'/'jumps') in the time evolution of the fundamental solution matrix. The jumps occur when the trajectory crosses a hypersurface of discontinuity. The trajectory $\underset{\sim}{x}(t)$ is continuous in time, but the right-hand side $\underset{\sim}{f}(t, \underset{\sim}{x})$ is discontinuous on the hypersurface, which causes a jump in the fundamental solution matrix. The jump can be described by a saltation matrix $\underline{S}$

$$\underline{\Phi}(t_{p+}, t_0) = \underline{S}\, \underline{\Phi}(t_{p-}, t_0), \tag{10}$$

where $\underline{\Phi}(t_{p-}, t_0)$ is the fundamental solution matrix before the jump and $\underline{\Phi}(t_{p+}, t_0)$ after the jump which occurs at $t = t_p$. The saltation matrix $\underline{S}$ can be expressed as

$$\underline{S} = \underline{I} + \frac{\left(\underset{\sim}{f}_{p+} - \underset{\sim}{f}_{p-} \right) \underset{\sim}{n}^\top}{\underset{\sim}{n}^\top \underset{\sim}{f}_{p-} + \frac{\partial h}{\partial t}\left(t_p, \underset{\sim}{x}(t_p)\right)}, \tag{11}$$

where $\underset{\sim}{n}$ is the normal to the hypersurface

$$\underset{\sim}{n} = \underset{\sim}{n}\left(t, \underset{\sim}{x}(t)\right) = \operatorname{grad}\left(h\left(t, \underset{\sim}{x}(t)\right)\right). \tag{12}$$

The construction of saltation matrices is due to Aizerman and Gantmakher [39] and treated in [26,40–42]. The saltation matrices for each hypersurface are

$$\underline{S}_{1a} = \begin{bmatrix} 1 & 0 \\ -\dfrac{c_f}{m} & 1 \end{bmatrix}, \tag{13}$$

$$\underline{S}_{1b} = \underline{I}, \tag{14}$$

$$\underline{S}_{2a} = \begin{bmatrix} 1 & 0 \\ -\dfrac{c_f}{m} & 1 \end{bmatrix}, \tag{15}$$

$$\underline{S}_{2b} = \underline{I}. \tag{16}$$

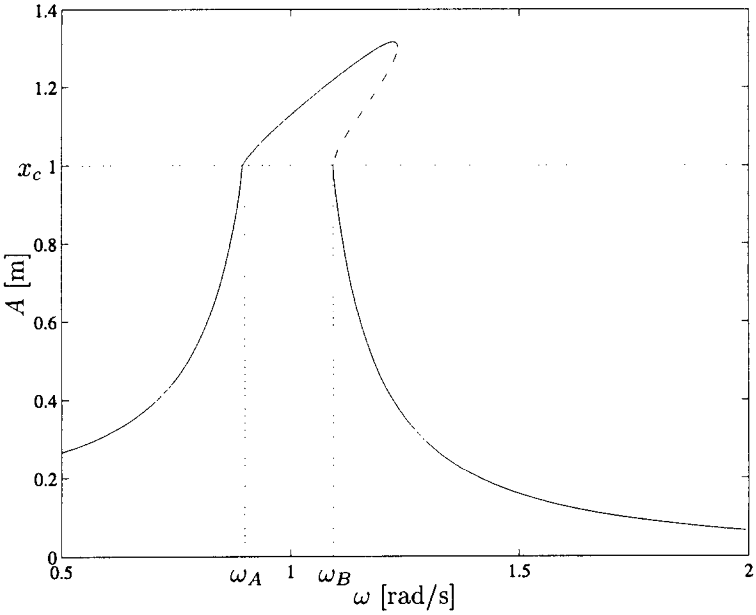

Figure 4. Response diagram of trilinear spring system.

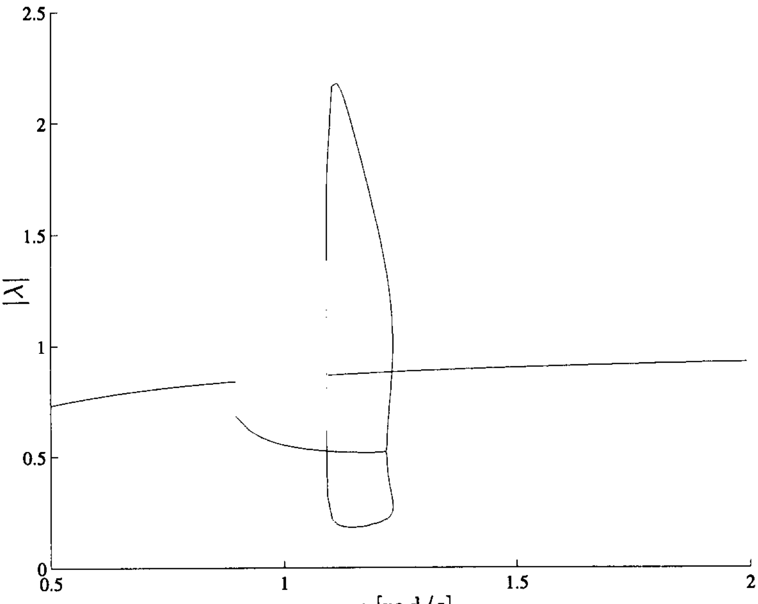

Figure 5. Floquet multipliers.

The hypersurfaces Σ_1 and Σ_2 are nonsmooth. The saltation matrices are not each other's inverse, $\underline{S}_{1a} \neq \underline{S}_{1b}^{-1}$ and $\underline{S}_{2a} \neq \underline{S}_{2b}^{-1}$. This will turn out to be essential for the existence of a discontinuous bifurcation. Note that the saltation matrices are independent of the stiffness k_f and reduce to the identity matrix if $c_f = 0$.

The response diagram of the trilinear system is shown in Figure 4 for varying forcing frequencies with the amplitude A of x on the vertical axis. Stable branches are indicated by solid lines and unstable branches by dashed-dotted lines. The parameter values are given in Appendix A.

There is no contact with the support for amplitudes smaller than x_c and the response curve is just the linear harmonic peak. For amplitudes above x_c, there will be contact with the support, which will cause a hardening behaviour of the response curve. The backbone curve of the peak bends to the right like the Duffing system with a hardening spring. The amplitude becomes equal to x_c twice at $\omega = \omega_A$ and $\omega = \omega_B$, on both sides of the peak, and corners of the response curve can be seen at these points. The orbit touches the corners of Σ_1 and Σ_2 for $A = x_c$.

The magnitude of the Floquet multipliers is shown in Figure 5. The two Floquet multipliers are complex conjugate (with the same magnitude) for $A < x_c$. The orbit touches the two hypersurfaces at $A < x_c$, and the fundamental solution matrix will jump as follows from the saltation matrices. The eigenvalues of the fundamental solution matrix, which are known as the Floquet multipliers, will therefore jump (indicated by dotted lines in Figure 5). The Floquet multipliers are not single valued at the bifurcation point (as is the case for smooth systems), but are set-valued.

The pair of Floquet multipliers jumps at ω_A but does not jump through the unit circle. The set-valued Floquet multiplier remains within the unit circle. The stable branch therefore remains stable. However, at $\omega = \omega_B$ the complex pair jumps to two distinct real multipliers, one with a magnitude bigger than one. Hence, one of those Floquet multipliers therefore jumps through the unit circle. This set-valued Floquet multiplier passed the unit circle through $+1$ causing a *discontinuous fold bifurcation.*

Damping of the support is essential for the existence of this discontinuous fold bifurcation. For $c_f = 0$, all saltation matrices would be equal to the identity matrix and the corner between Σ_{1a} and Σ_{1b} would disappear (and also between Σ_{2a} and Σ_{2b}). Consequently, no discontinuous bifurcation could take place, and the fold bifurcation would be smooth. The model of Natsiavas [37,38] did not contain a *discontinuous* fold bifurcation because the transitions were modeled such that $\underline{S}_{1a} = \underline{S}_{1b}^{-1}$ and $\underline{S}_{2a} = \underline{S}_{2b}^{-1}$. The saltation matrices will cancel out each other if they are each other's inverse. A corner of hypersurfaces with saltation matrices which are not each other's inverse is therefore essential (but not sufficient) for the existence of a discontinuous bifurcation.

3. STICK-SLIP SYSTEM

In the preceding section, we studied a discontinuous fold bifurcation, where a Floquet multiplier jumped through the unit circle to a finite value. In this section, we will study a discontinuous fold bifurcation where a Floquet multiplier jumps to infinity. This results in an infinitely unstable periodic solution.

We consider the block-on-belt model depicted in Figure 6 with the parameter values given in Appendix B. The state equation of this autonomous system reads

$$\dot{\underset{\sim}{x}} = \underset{\sim}{f}(\underset{\sim}{x}) = \begin{bmatrix} \dot{x} \\ -\frac{k}{m}x - \frac{c}{m}\dot{x} + \frac{F}{m} \end{bmatrix}, \tag{17}$$

where $\underset{\sim}{x} = [x \quad \dot{x}]^{\top}$, and the friction force F is given by

$$F(v_{\text{rel}}, x) = \begin{cases} -F_{\text{slip}} \operatorname{sgn} v_{\text{rel}}, & v_{\text{rel}} \neq 0, \text{ slip}, \\ \min\left(|kx + c\dot{x}|, F_{\text{stick}}\right) \operatorname{sgn} kx, & v_{\text{rel}} = 0, \text{ stick}. \end{cases} \tag{18}$$

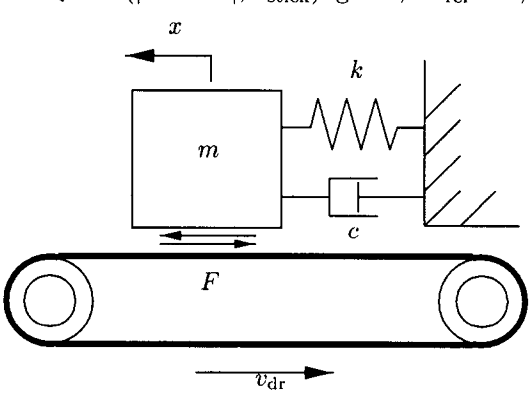

Figure 6. 1-DOF model with dry friction.

The maximum static friction force is denoted by F_{stick} and $v_{\text{rel}} = \dot{x} - v_{\text{dr}}$ is the relative velocity. The constitutive relation for F is the known as the *signum model with static friction point*.

This model permits analytical solutions for $c = 0$ due to its simplicity, but it is not directly applicable in numerical analysis. The relative velocity will most likely not be exactly zero in digital computation. Instead, an adjoint *switch model* [41,43] will be studied which is discontinuous but yields a set of ordinary (and nonstiff!) differential equations. The state equation for the switch model reads

$$\dot{\underset{\sim}{x}} = \begin{cases} \begin{bmatrix} \dot{x} \\ -\dfrac{k}{m}x - \dfrac{c}{m}\dot{x} - \dfrac{F_{\text{slip}}}{m}\operatorname{sgn} v_{\text{rel}} \end{bmatrix}, & |v_{\text{rel}}| > \eta \text{ or } |kx + c\dot{x}| > F_{\text{stick}}, \\ \begin{bmatrix} v_{\text{dr}} \\ -v_{\text{rel}}\sqrt{\dfrac{k}{m}} \end{bmatrix}, & |v_{\text{rel}}| < \eta \text{ and } |kx + c\dot{x}| < F_{\text{stick}}. \end{cases} \tag{19}$$

A region of near-zero velocity is defined as $|v_{\text{rel}}| < \eta$ where $\eta \ll v_{\text{dr}}$. The space $\mathbb{R}^2$ is divided in three subspaces V, W, and D as indicated in Figure 7. The small parameter η is enlarged to make D visible.

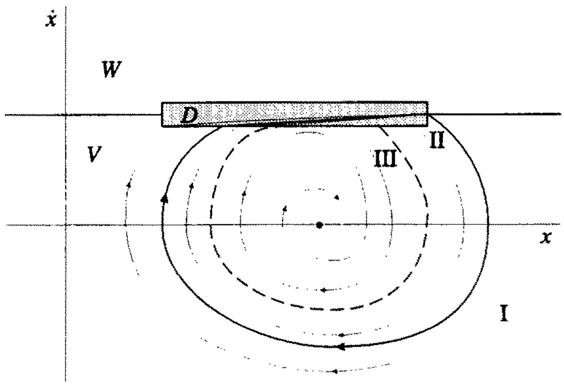

Figure 7. Phase plane.

The equilibrium solution of system (17) is given by

$$\underset{\sim}{x}_{\text{eq}} = \begin{bmatrix} \dfrac{F_{\text{slip}}}{k} \\ 0 \end{bmatrix} \tag{20}$$

and is stable for positive damping ($c > 0$).

The model also exhibits stable periodic stick-slip oscillations. The saltation matrix $\underset{\sim}{S}_\alpha$ for the transition from slip to stick is given by [41]

$$\underset{\sim}{S}_\alpha = \begin{bmatrix} 1 & 0 \\ 0 & 0 \end{bmatrix}, \tag{21}$$

which is singular. The fundamental solution matrix will therefore also be singular as the stable periodic oscillation passes the stick state. The saltation matrix $\underset{\sim}{S}_\beta$ for the transition from stick to slip is given by

$$\underset{\sim}{S}_\beta = \begin{bmatrix} 1 & 0 \\ -\dfrac{\Delta F}{m v_{\text{dr}}} & 1 \end{bmatrix}, \tag{22}$$

with $\Delta F = F_{\text{stick}} - F_{\text{slip}}$.

The periodic solution has two Floquet multipliers, of which one is always equal to unity as the system is autonomous. The singularity of the fundamental solution matrix implies that the remaining Floquet multiplier has to be equal to zero, independent of any system parameter. The Floquet multipliers of the stable periodic solution of this system are therefore 1 and 0.

The stable limit cycle is sketched in the phase plane in Figure 7 (bold line). The equilibrium position is also stable and indicated by a dot. The space D is enlarged in Figure 7 to make it visible, but is infinitely small in theory and is taken very small in numerical calculations [41,43].

A trajectory outside the stable limit cycle, like Trajectory I in Figure 7, will spiral inwards to the stable limit cycle and reach the stick-phase D. The stick-phase will bring the trajectory exactly on the stable limit cycle as it is infinitely small. Every point in D is therefore part of the basin of attraction of the stable limit cycle.

Trajectory II starts inside the stable limit cycle and spirals around the equilibrium position and hits D whereafter it is on the stable limit cycle. But a trajectory inside the stable limit cycle might also spiral around the equilibrium position and not reach the stick phase D (Trajectory III). It will then be attracted to the equilibrium position.

A trajectory inside the stable limit cycle can therefore spiral outwards to the stable limit cycle, like Trajectory II, or inwards to the equilibrium position (Trajectory III). Consequently, there must exist a separating boundary of between the two attracting limit sets. This boundary is the unstable limit cycle sketched by a dashed line in Figure 7. Whether a trajectory is attracted to the stable limit cycle or to the equilibrium point depends on the attainment of the trajectory to D. The unstable limit cycle is therefore defined by the trajectory in V which hits the border of D tangentially. Another part of the unstable limit cycle is along the border of D as trajectories in D will attract to the stable limit cycle and just outside D to the equilibrium position. This part of the unstable limit cycle along the the border of D has a vector field which is repulsing on both sides of the border. The theory of Filippov gives a generalized solution of systems with a discontinuous right-hand side [25,26,41]. If the vector field on one side of a hypersurface of discontinuity is pushing to the hypersurface and on the other side from the hypersurface, then every trajectory will intersect the hypersurface transversally. If the vector field is pushing to the hypersurface on both sides, then there exists a unique solution along the hypersurface. This is called an *attraction sliding mode*. If the vector field is repulsing from both sides of the hypersurface, then there exists a solution along the hypersurface which is not unique. This is called a *repulsion sliding mode*.

The trajectory on either side of the border of D is repulsing from it. It is therefore a repulsion sliding mode. The trajectory starting from a point on a repulsion sliding mode is not unique as follows from the theory of Filippov. This causes the unstable solution to be infinitely unstable. As the trajectory is infinitely unstable, it is not possible to calculate it in forward time. However, calculation of the trajectory in backward time is possible. The vector field in backward time is identical to the one in forward time, but opposite in direction. The repulsion sliding mode in forward time will turn into an attraction sliding mode in backward time. The trajectory starting from a point on the unstable limit cycle will move counterclockwise in the phase-plane in backward time and hit the border of D. It will slide along the border of D until the vector field in V becomes parallel to D, and will then bend off in V. Any trajectory starting from a point close to that starting point will hit D and leave D at exactly the same point. Information about where the trajectory came from is therefore lost through the attraction sliding mode. In other words, the saltation matrix of the transition from V to D during backward time is singular. The fundamental solution matrix will therefore be singular in backward time because it contains an attraction sliding mode. The Floquet multipliers of the unstable limit cycle in backward time are therefore 1 and 0. The Floquet multipliers in forward time must be their reciprocal values. The second Floquet multiplier is therefore infinity, which of course must hold for an infinitely unstable periodic solution.

The bifurcation diagram of the system is shown in Figure 8 with the velocity of the belt v_{dr} as parameter and the amplitude A on the vertical axis. The equilibrium branch and the stable

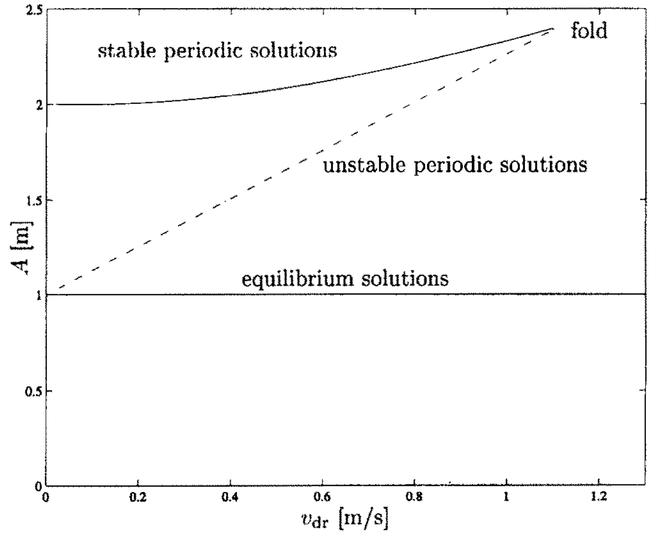

Figure 8. Bifurcation diagram of the block-on-belt model.

and unstable periodic branches are depicted. The unstable branch is of course located between the stable periodic branch and the equilibrium branch as can be inferred from Figure 7. The stable and unstable periodic branches are connected through a fold bifurcation point. The second Floquet multiplier jumps from $\lambda = 0$ to $\lambda = \infty$ at the bifurcation point. This set-valued Floquet multiplier therefore passes the unit circle at +1. The fold bifurcation is therefore a discontinuous fold bifurcation. The fold bifurcation occurs when v_{dr} is such that a trajectory which leaves the stick phase D, transverses V, and hits D tangentially (like the unstable periodic solution). The stable and unstable periodic solutions coincide at this point. Note that there exists again a corner of hypersurfaces at this point as was the case in the previous section. The saltation matrices are not each others inverse, $\underline{S}_\alpha \underline{S}_\beta \neq \underline{I}$, which is essential for the existence of a discontinuous bifurcation.

A similar model was studied by Van de Vrande *et al.* [20] with a very accurately smoothed friction curve. The stable branch was followed for increasing v_{dr}, but the fold bifurcation could not be rounded to proceed on the unstable branch. As the unstable branch is infinitely unstable in theory, it is extremely unstable for the smoothed system. The branch can therefore not be followed in forward time if the friction model is approximated accurately.

The stable branch in Figure 8 was followed in forward time up to the bifurcation point. The path-following algorithm was stopped and restarted in backward time to follow the unstable branch.

This section showed that infinitely unstable periodic solutions come into being through repulsion sliding modes. Filippov's theory turns out to be essential for the understanding of infinitely unstable periodic solutions. Infinitely unstable periodic solutions and their branches can be found through backward integration. Smoothing of a discontinuous model is not sufficient to obtain a complete bifurcation diagram of a discontinuous system as infinitely unstable branches cannot be found.

4. SYMMETRY-BREAKING BIFURCATION; FORCED VIBRATION WITH DRY FRICTION

The second type of bifurcation of a periodic solution which will be studied in this paper is the *symmetry-breaking bifurcation*. Suppose a nonautonomous time-periodic system has the following symmetry property (also called *inversion symmetry*):

$$\underset{\sim}{f}(t, \underset{\sim}{x}) = -\underset{\sim}{f}\left(t + \frac{1}{2}T, -\underset{\sim}{x}\right), \tag{23}$$

where T is the period. If $\underset{\sim}{x}_1(t) = \underset{\sim}{x}(t)$ is a periodic solution of the system, then also $\underset{\sim}{x}_2(t) = -\underset{\sim}{x}(t + (1/2)T)$ must be a periodic solution. The periodic solution is called *symmetric* if $\underset{\sim}{x}_1(t) = \underset{\sim}{x}_2(t)$ and asymmetric if $\underset{\sim}{x}_1(t) \neq \underset{\sim}{x}_2(t)$. When a Floquet multiplier crosses the unit circle through $+1$, the associated bifurcation depends on the nature of the periodic solution prior to the bifurcation. Suppose that the periodic solution prior to the bifurcation is a symmetric solution. Then, if the bifurcation breaks the symmetry of the periodic solution, it is called a symmetry-breaking bifurcation [35].

We will show in this section that symmetry-breaking bifurcations can also be discontinuous. Consider the forced vibration of the system depicted in Figure 9. The mass is supported by a spring, damper, and dry friction element. The parameter values are given in Appendix C. The equation of motion reads

$$m\ddot{x} + c\dot{x} + kx = f_{\text{fric}}(\dot{x}, x) + f_0 \cos \omega t \tag{24}$$

with the friction model

$$f_{\text{fric}}(\dot{x}, x) = \begin{cases} -F_{\text{slip}} \operatorname{sgn}(\dot{x}), & \dot{x} \neq 0, \text{ slip}, \\ \min\left(|kx - f_0 \cos \omega t|, F_{\text{stick}}\right) \operatorname{sgn}(kx - f_0 \cos \omega t), & \dot{x} = 0, \text{ stick}. \end{cases} \tag{25}$$

It can be verified that this system has the symmetry property (23).

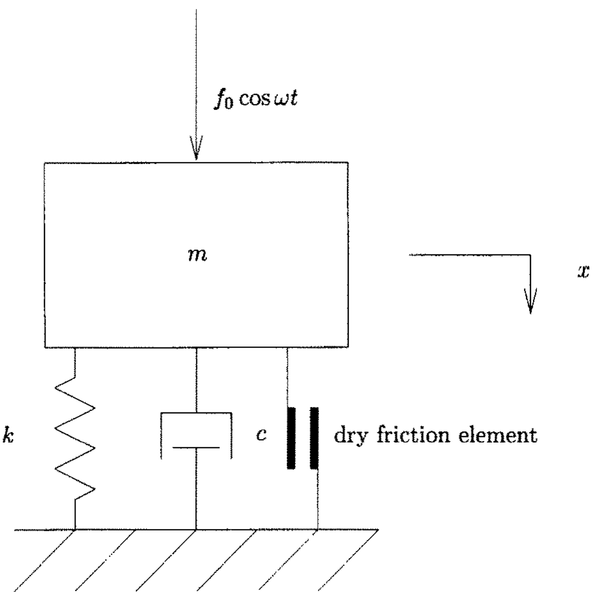

Figure 9. Forced vibration with dry friction.

The bifurcation diagram of this system is depicted in Figure 10 and consists of a Branch I which is partly unstable (between the points A and B) and Branch II which bifurcates from Branch I. For large amplitudes, the influence of the dry friction element will be much less than the linear elements. Near the resonance frequency, $\omega_{\text{res}} = \sqrt{k/m} = 1$ [rad/s], Branch I will therefore be close to the harmonic resonance peak of a linear one degree-of-freedom system. We first consider periodic solutions on Branch I at the right side of point B. The velocity of the mass $\dot{x}$ becomes zero at two instances of time during one oscillation (as do linear harmonic oscillations). The mass does not come to a stop during an interval of time. In other words, the oscillation contains no *stick event* in which the trajectory passes the stick phase. The number of stick events on a part of a branch is indicated by numbers $(0, 1, 2)$ in Figure 10. The Floquet multipliers on this

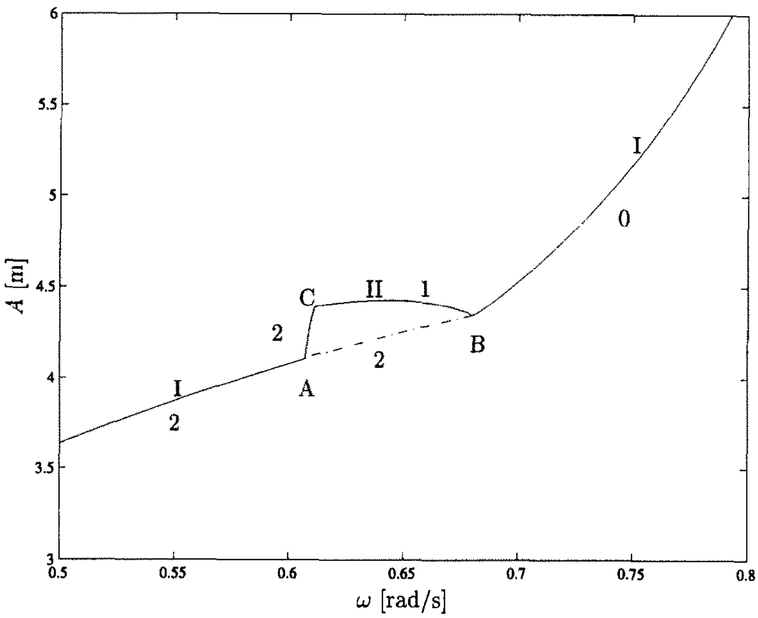

Figure 10. Bifurcation diagram of forced vibration with dry friction.

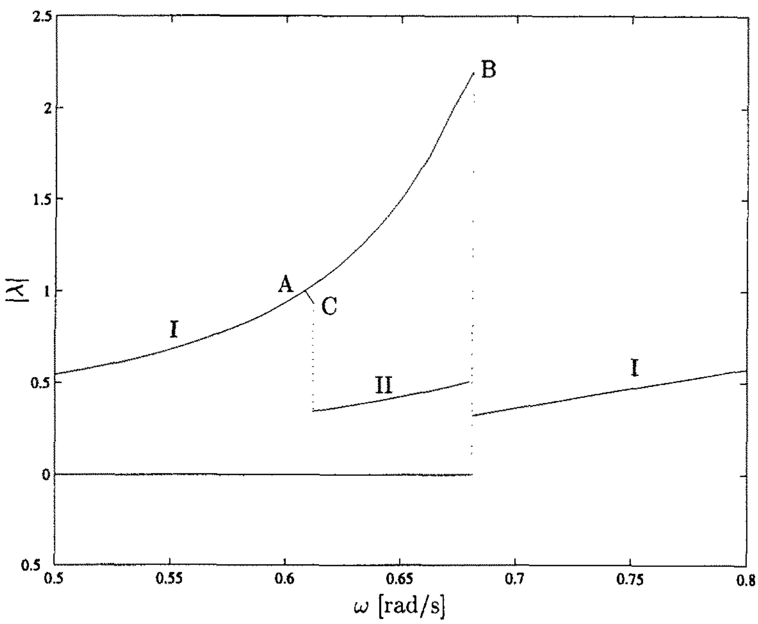

Figure 11. Floquet multipliers.

part of Branch I are complex (Figure 11). The system therefore behaves 'almost linearly'. All the periodic solutions on Branch I are symmetric.

If this part of Branch I with 'almost linear' symmetric solutions is followed to frequencies below ω_{res}, then bifurcation point B is met. At bifurcation point B, the symmetric Branch I becomes unstable, and a second Branch II with asymmetric solutions is created. In fact, on the bifurcated asymmetric branch, two distinct solutions $\underset{\sim}{x}_1(t) \neq \underset{\sim}{x}_2(t)$ exist, which have the same amplitude. The solutions on Branch I left of point B contain two stick events per cycle. The solutions on Branch II between the points B and C contain one stick event, and they contain two stick events between the points A and C. The existence of a stick event during the oscillation causes one Floquet multiplier to be equal to zero. Points B and C are points where stick events are created/destroyed, which cause the Floquet multipliers to be set-valued (they jump). A set-valued Floquet multiplier at B passes +1. Point B is therefore a *discontinuous symmetry-breaking bifurcation*.

Branch II encounters a jump of the Floquet multipliers at point C, but the set-valued Floquet multipliers remain within the unit circle. Point C is therefore not a bifurcation point, but the path of Branch II is nonsmooth at C due to the jump of the Floquet multipliers.

The asymmetric branch meets the symmetric branch again at point A. The Floquet multipliers pass +1 without a jump, and point A is therefore a continuous symmetry bifurcation. No stick events are created at point A because all branches have two stick events per cycle. Remark that the Branch I behaves smooth at bifurcation A and nonsmooth at bifurcation B.

5. CONCLUSIONS

It was shown in this paper that discontinuous vector fields lead to jumps in the fundamental solution matrix if a parameter of the system is varied. It turned out that a double intersection of a nonsmooth hypersurface is necessary to cause a jump of the fundamental solution matrix. These jumps may lead to set-valued Floquet multipliers. A discontinuous bifurcation is encountered if a set-valued Floquet multiplier crosses the unit circle.

An example with a trilinear spring demonstrated two jumps of the Floquet multipliers, one causing a discontinuous fold bifurcation.

An example of a stick-slip system showed that the Floquet multiplier can also jump to infinity. The discontinuous fold bifurcation connects a stable branch to an infinitely unstable branch. The unstable limit cycle can be understood by Filippov's theory. Infinitely unstable periodic solutions come into being through repulsion sliding modes and can be found through backward integration. Branches of infinitely unstable periodic solutions can be continued with pseudoarclength continuation based on shooting with backward integration. Bifurcation to infinitely unstable periodic solutions lead to complete failure of the classical smoothing method to investigate discontinuous systems.

A continuous and a discontinuous symmetry-breaking bifurcation were shown to exist in a mass-spring-damper system with dry friction.

Different aspects of discontinuous bifurcations have been shown in this paper. Only fold and symmetry-breaking bifurcations were discussed. A more complete treatment of bifurcations in discontinuous systems is presented in [41,44].

APPENDIX A
TRILINEAR SPRING SYSTEM

$$
\begin{aligned}
&m = 1\,\mathrm{kg}, && c = 0.05\,\frac{\mathrm{Ns}}{\mathrm{m}}, && k = 1\,\frac{\mathrm{N}}{\mathrm{m}}, && x_c = 1\,\mathrm{m},\\
&k_f = 4\,\frac{\mathrm{N}}{\mathrm{m}}, && c_f = 0.5\,\frac{\mathrm{Ns}}{\mathrm{m}}, && f_0 = 0.2\,\mathrm{N}.
\end{aligned}
$$

APPENDIX B
STICK-SLIP SYSTEM

$$
\begin{aligned}
&k = 1\,\frac{\mathrm{N}}{\mathrm{m}}, && c = 0.1\,\frac{\mathrm{Ns}}{\mathrm{m}}, && m = 1\,\mathrm{kg}, && v_{\mathrm{dr}} = 0 \cdots 1.3\,\frac{\mathrm{m}}{\mathrm{s}},\\
&F_{\mathrm{slip}} = 1\,\mathrm{N}, && F_{\mathrm{slip}} = 2\,\mathrm{N}, && \eta = 10^{-4}\,\frac{\mathrm{m}}{\mathrm{s}}.
\end{aligned}
$$

APPENDIX C

FORCED VIBRATION WITH DRY FRICTION

$$m = 1\,\text{kg}, \qquad c = 0.01\,\frac{\text{Ns}}{\text{m}}, \qquad k = 1\,\frac{\text{N}}{\text{m}},$$
$$f_0 = 2.5\,\text{N}, \qquad F_{\text{slip}} = 1\,\text{N}, \qquad F_{\text{stick}} = 2\,\text{N}.$$

REFERENCES

1. J. Guckenheimer and P. Holmes, *Nonlinear Oscillations, Dynamical Systems, and Bifurcations of Vector Fields, Applied Mathematical Sciences 42*, Springer-Verlag, New York, (1983).
2. P. Hagedorn, *Non-Linear Oscillations, Oxford Engineering Science Series 10*, Clarendon Press, Oxford, (1988).
3. Y.A. Kuznetsov, *Elements of Applied Bifurcation Theory, Applied Mathematical Sciences 112*, Springer-Verlag, New York, (1995).
4. R. Seydel, *Practical Bifurcation and Stability Analysis; From Equilibrium to Chaos, Interdisciplinary Applied Mathematics*, Springer-Verlag, New York, (1994).
5. C.J. Begley and L.N. Virgin, A detailed study of the low-frequency periodic behavior of a dry friction oscillator, *Journal of Dynamic Systems, Measurement, and Control* **119**, 491–497, (1997).
6. C.J. Begley and L.N. Virgin, Impact response under the influence of friction, *Journal of Sound and Vibration* **211** (5), 801–818, (1998).
7. B. Blazejczyk-Okolewska and T. Kapitaniak, Dynamics of impact oscillator with dry friction, *Chaos, Solitons and Fractals* **7** (9), 1455–1459, (1996).
8. U. Galvanetto, S.R. Bishop and L. Briseghella, Mechanical stick-slip vibrations, *International Journal of Bifurcation and Chaos* **5** (3), 637–651, (1995).
9. U. Galvanetto and C. Knudsen, Event maps in a stick-slip system, *Nonlinear Dynamics* **13** (2), 99–115, (1997).
10. N. Hinrichs, Reibsschwingungen mit Selbst- und Fremderregung: Experiment, Modellierung und Berechnung, Fortschr.-Ber. VDI Reihe 11, Nr. 240, VDI Verlag, Düsseldorf, (1997).
11. N. Hinrichs, M. Oestreich and K. Popp, On the modelling of friction oscillators, *Journal of Sound and Vibration* **216** (3), 435–459, (1998).
12. R.A. Ibrahim, Friction-induced vibration, chatter, squeal and, chaos; Part I: Mechanics of contact and friction, *ASME Applied Mechanics Reviews* **47** (7), 209–226, (1994).
13. R.A. Ibrahim, Friction-induced vibration, chatter, squeal and, chaos; Part II: Dynamics and modeling, *ASME Applied Mechanics Reviews* **47** (7), 227–253, (1994).
14. M. Kunze and T. Küpper, Qualitative bifurcation analysis of a non-smooth friction oscillator model, *ZAMP* **48** (1), 87–101, (1997).
15. K. Popp, Some model problems showing stick-slip motion and chaos, In *ASME WAM, Proc. Symp. on Friction Induced Vibration, Chatter, Squeal, and Chaos, Volume 49*, (Edited by R.A. Ibrahim and A. Soom), pp. 1–12, ASME, New York, (1992).
16. K. Popp, N. Hinrichs and M. Oestreich, Dynamical behaviour of a friction oscillator with simultaneous self and external excitation, In *Sādhanā: Academy Proceedings in Engineering Sciences, Part 2-4, Volume 20*, pp. 627–654, Indian Academy of Sciences, Banglore, India, (1995).
17. E. Reithmeier, *Periodic Solutions of Nonlinear Dynamical Systems*, Springer-Verlag, Berlin, (1991).
18. P. Stelter, Nonlinear vibrations of structures induced by dry friction, *Nonlinear Dynamics* **3**, 329–345, (1992).
19. P. Stelter and W. Sextro, Bifurcations in dynamical systems with dry friction, *International Series of Numerical Mathematics* **97**, 343–347, (1991).
20. B.L. Van de Vrande, D.H. Van Campen and A. De Kraker, An approximate analysis of dry-friction-induced stick-slip vibrations by a smoothing procedure, *Nonlinear Dynamics* **19** (2), 157–169, (1999).
21. M. Wiercigroch, On modelling discontinuities in dynamic systems, *Machine Vibration* **5**, 112–119, (1996).
22. Y. Yoshitake and A. Sueoka, Forced self-exited vibration accompanied by dry friction, In *Applied Nonlinear Dynamics and Chaos of Mechanical Systems with Discontinuities*, (Edited by M. Wiercigroch and A. de Kraker), World Scientific (to appear).
23. Y. Yoshitake, A. Sueoka, N. Shoji and T. Hai, Vibrations of nonlinear systems with discontinuities, The case of the preloaded compliance system, *JSME Series C* **41** (4), 710–717, (1998).
24. A.A. Andronov, A.A. Vitt and S.E. Khaikin, *Theory of Oscillators*, Reprint, Dover Publications, New York, (1987); Originally translated from Russian, Pergamon Press, Oxford, (1966).
25. A.F. Filippov, Differential equations with discontinuous right-hand side, *American Mathematical Society Translations, Series 2* **42**, 199–231, (1964).
26. A.F. Filippov, Differential equations with discontinuous right-hand sides, In *Mathematics and Its Applications*, Kluwer Academic, Dordrecht, (1988).
27. B. Brogliato, *Nonsmooth Mechanics*, Springer, London, (1999).

28. M.I. Feigin, On the generation of sets of subharmonic modes in a piecewise-continuous system, *PMM* **38** (5), 810–818, (1974).
29. M.I. Feigin, On the structure of C-bifurcation boundaries of piece-wise continuous systems, *PMM* **42** (5), 820–829, (1978).
30. M.I. Feigin, The increasingly complex structure of the bifurcation tree of a piecewise-smooth system, *Journal of Applied Mathematics and Mechanics* **59** (6), 853–863, (1995).
31. M. di Bernardo, M.I. Feigin, S.J. Hogan and M.E. Homer, Local analysis of C-bifurcations in n-dimensional piecewise-smooth dynamical systems, *Chaos, Solitons and Fractals* **10** (11), 1881–1908, (1999).
32. M. di Bernardo, K. Johansson and F. Vasca, Sliding orbits and their bifurcations in relay feedback systems, In *Proceedings of the 38th Conference on Design & Control*, Phoenix, December 1999, CD-ROM publication, pp. 708–713, (1999).
33. M. di Bernardo, C. Budd and A. Champneys, Grazing, skipping and sliding: Analysis of the non-smooth dynamics of the DC/DC buck converter, *Nonlinearity* **11**, 859–890, (1998).
34. H.E. Nusse and J.A. York, Border-collision bifurcations including "period two to period three" for piecewise smooth systems, *Physica D* **57**, 39–57, (1992).
35. A.H. Nayfeh and B. Balachandran, *Applied Nonlinear Dynamics; Analytical, Computational, and Experimental Methods*, Wiley-International, Chichester, (1995).
36. A.H. Nayfeh and D.T. Mook, *Nonlinear Oscillations*, Wiley, New York, (1979).
37. S. Natsiavas, Periodic response and stability of oscillators with symmetric trilinear restoring force, *Journal of Sound and Vibration* **134** (2), 315–331, (1989).
38. S. Natsiavas and H. Gonzalez, Vibration of harmonically excited oscillators with asymmetric constraints, *ASME Journal of Applied Mechanics* **59**, 284–290, (1992).
39. M.A. Aizerman and F.R. Gantmakher, On the stability of periodic motions (translated from Russian), *Journal of Applied Mathematics and Mechanics*, 1065–1078, (1958).
40. S.F. Bockman, Lyapunov exponents for systems described by differential equations with discontinuous right-hand sides, *Proceedings of the American Control Conference*, pp. 1673–1678, (1991).
41. R.I. Leine, Bifurcations in nonlinear discontinuous systems, Ph.D. Thesis, Eindhoven University of Technology, The Netherlands, (June 2000).
42. P.C. Müller, Calculation of Lyapunov exponents for dynamic systems with discontinuities, *Chaos, Solitons and Fractals* **5** (9), 1671–1681, (1995).
43. R.I. Leine, D.H. Van Campen, A. De Kraker and L. Van den Steen, Stick-slip vibrations induced by alternate friction models, *Nonlinear Dynamics* **16** (1), 41–54, (1998).
44. R.I. Leine and D.H. Van Campen, Fold bifurcations in discontinuous systems, In *Proceedings of DETC'99 ASME Design Engineering Technical Conferences*, September 12–15, 1999, Las Vegas, CD-ROM, DETC99/VIB-8034, (1999).